First Results on Compton Camera Coincidences With the Silicon Drift Detector

Tuba Çonka-Nurdan, K. Nurdan, A. H. Walenta, I. Chiosa, B. Freisleben, N. A. Pavel, and L. Strüder

***Abstract*—A Compton camera system consisting of a silicon drift detector (SDD) and an Anger camera has been constructed to study coincidence events and the possibility of tracking a recoil electron. An event is considered as a coincidence when a photon emitted from a radioactive source is first Compton scattered in the SDD where the recoil electron deposits its energy and the scattered photon undergoes a photoelectric absorption in the NaI(Tl) crystal of the Anger camera. The SDD is composed of a monolithic array of 19 hexagonal cells each having an on-chip transistor which provides the first stage amplification. ^{137}Cs source has been finely collimated in order to study events occuring at different locations within a single cell. The equipment is designed such that the measurements can be done in all detector orientations and kinematical conditions. The angular and energy distribution of coincidence events have been studied with high statistics. Energy resolution and angle measurements performed with this detector system will be presented in this paper.**

***Index Terms*—Compton camera, gamma camera, silicon drift detector.**

I. Introduction

A COMPTON CAMERA is a promising imaging system in various fields like nuclear medicine [1], astrophysics [2], and industrial applications [3]. It usually consists of a scatter detector where the Compton scattering occurs and an absorption detector where the scattered photon is absorbed. Position and energy measurements in both detectors—with the help of well-known Compton kinematics—are used to reconstruct the location of the source which can lie anywhere on a surface of a cone whose axis and opening angle are defined by these measurements.

A detector system has been constructed to study the Compton events in a silicon drift detector [4], [5]. A silicon drift detector (SDD) with on-chip electronics was chosen for its excellent energy resolution and high rate capability. The analog and digital readout of the SDD [6] is achieved with a custom designed electronics. The Anger camera with its large NaI(Tl) crystal provides a large field of view for the scattered photons. Events that are time coincident in both detectors have been analyzed further to study the energy and angular distribution. Among those events, detailed analysis of SDD events can deliver more information about the track of the recoil electron, which deposits partial energy in several detector cells.

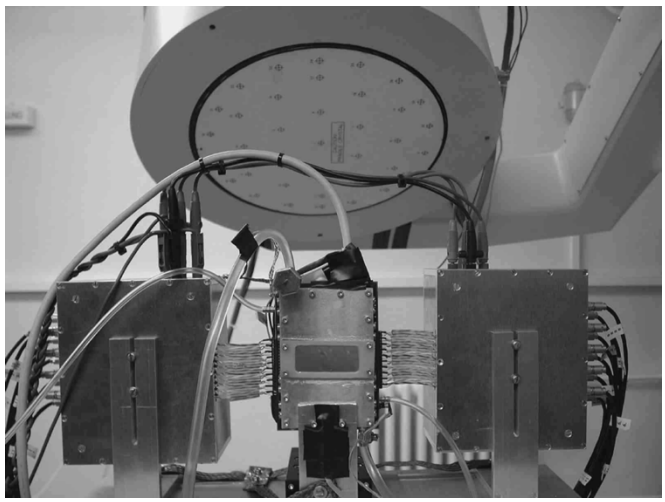

Fig. 1. The Compton camera test setup consisting of a silicon drift detector as a scatter detector and an Anger camera as an absorption detector.

II. System Overview

The detector system [7] for studying the Compton coincidences is shown in Fig. 1. ^{137}Cs source was collimated down to a sub-mm scale to study events occuring at different locations of a single cell. Both detectors are located on a computer-controlled motor system in order to study different kinematical events.

The SDD chip has a thickness of 300 μm and a total effective area of about 95 mm^2. Each SDD cell has an hexagonal shape with an active area of 5 mm^2 and the distance between the centers of two contiguous cells is 2.4 mm. The readout was designed such that the on-chip junction field-effect-transistor is followed by another emitter follower stage in order to use a short shaping time. The front-end electronics consists of a low-noise preamplifier followed by a fast shaper and the shaped signals are digitized at a custom-designed data acquisition system where the operations like time stamping, peak finding, and integration are performed and trigger logic is applied to filter the useful events [8], [13]. An average equivalent noise charge of 40 electrons rms (corresponding to an energy resolution of 340 eV FWHM) was measured at 10 °C with a shaping time of 100 ns [9]. The

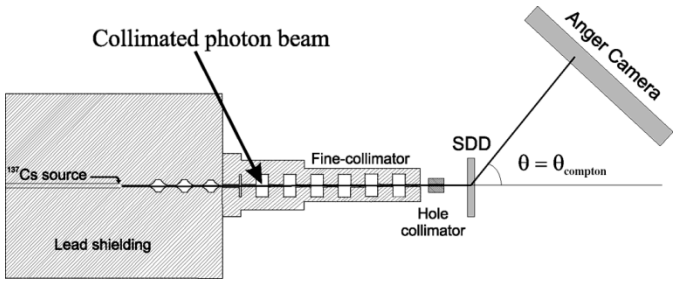

Fig. 2. The collimator setup for the 1-Ci ^{137}Cs source.

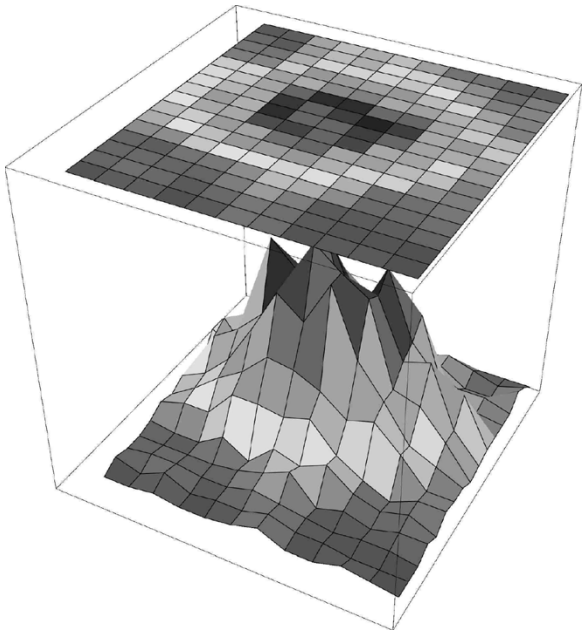

Fig. 3. x-y scan of a single SDD cell in 400 μm steps with 662 keV photons of ^{137}Cs source.

Anger camera consists of a 3/8-in-thick NaI(Tl) crystal which is coupled to 37 photomultiplier tubes.

A point-like ^{137}Cs placed in the main collimator is collimated further with a lead block having a 400-μm diameter hole as shown in Fig. 2. The beam spread measured at the location of the SDD is only 550 μm which enables to perform measurements by directing the beam at different positions within a single cell of the SDD.

Fig. 3 shows the x-y scan of a single cell with 662 keV photons. The number of events was recorded for each position only for a minute and the form of a cell is still clearly visible despite low statistics. The accuracy of the collimation is also proven with this result.

The difference between the time stamps of SDD and Anger camera events has been analyzed as a function of the drift field in the silicon detector. It was observed that it would be possible to discriminate the events occuring in the middle of a cell from those occuring at the edge of a cell when the drift field is much lower than usual with the expense of the energy resolution. In this way, it would be possible to tradeoff additional position resolution for energy resolution with the ultimate goal being the ability to track the recoil electron. Fig. 4 shows the variation of

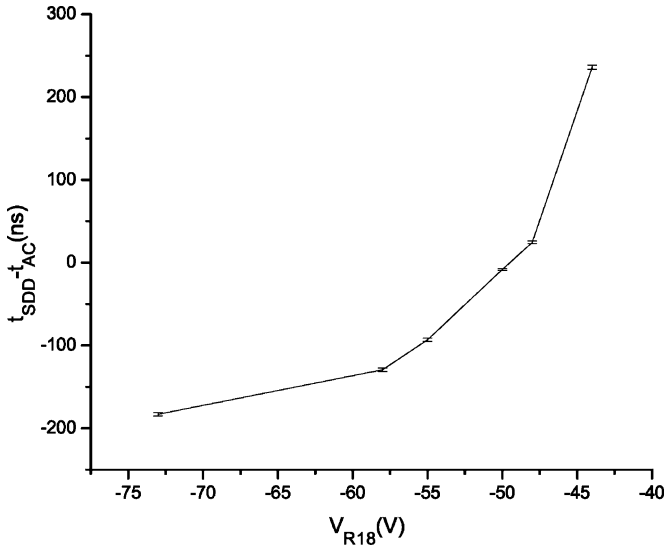

Fig. 4. The variation of the time stamp difference between the two detectors as a function of the drift field in the SDD.

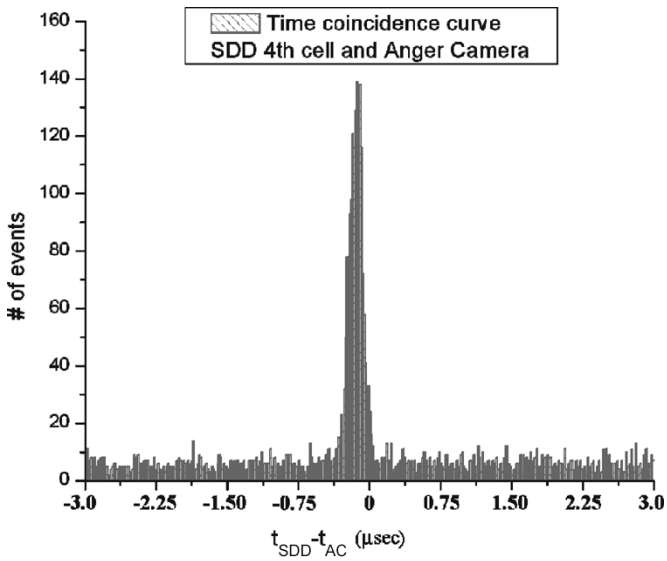

Fig. 5. Time coincidence curve for the coincident events occuring in the SDD and the Anger camera.

the mean time stamp difference as a function of a drift voltage for the events occuring away from the anode.

III. Coincidence Measurements

The recent measurements have been performed to gather high statistics of coincidence events for systematic analysis of the energy and the angular distributions of these events. The first measurements have been performed with the hole collimator placed in front of the fine collimator. The position of the SDD was adjusted such that the beam hits the center of a single SDD cell. The time coincidence curve obtained using the time stamp information from both detectors is shown in Fig. 5.

The FWHM value of the time coincidence distribution is around 250 ns which mainly results from the drift time of the electrons in the SDD. Although a wide region of time coincidences are scanned, most of the events concentrate in the

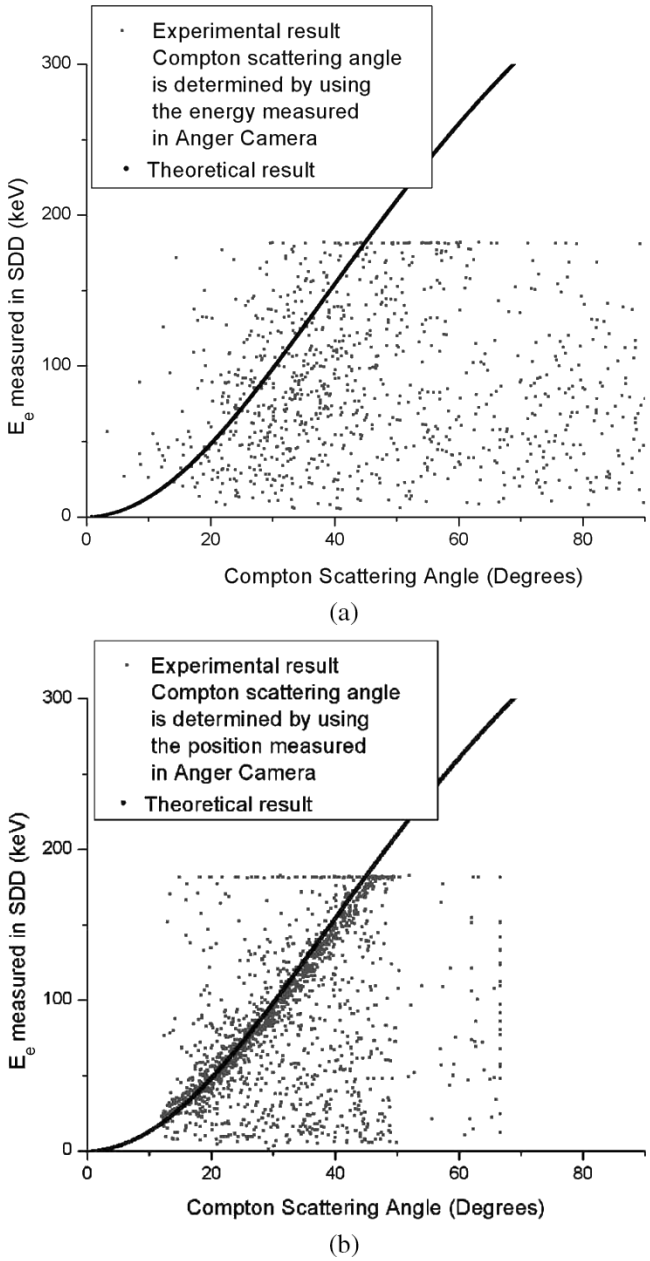

Fig. 6. The energy of the recoil electron measured in the SDD as a function of the Compton scattering angle which is calculated (a) using the energy measured in the Anger camera and (b) coordinate measured in the Anger camera.

region where $-300\ \mathrm{ns} < t_{\mathrm{SDD}} - t_{\mathrm{AC}} < 75\ \mathrm{ns}$. Leading-edge threshold is used for these measurements and the contribution of the time-walk to the overall timing uncertainty is around 30 ns. The events located in this region are selected for further analysis. Electron energy (E_e) distribution as a function of the Compton scattering angle which is calculated from the energy measured in the absorption detector (E_γ) with the theoretical expectation curve is shown in Fig. 6(a). The distribution does not really show a pattern similar to the theoretical curve due to the large energy uncertainty in the Anger camera. However, with the fine collimation of the beam which has an angular spread of only 0.03°, we can assume that the incoming photons are directed perpendicularly to the surface of the SDD. In this case, the Compton scattering angle can be measured using the

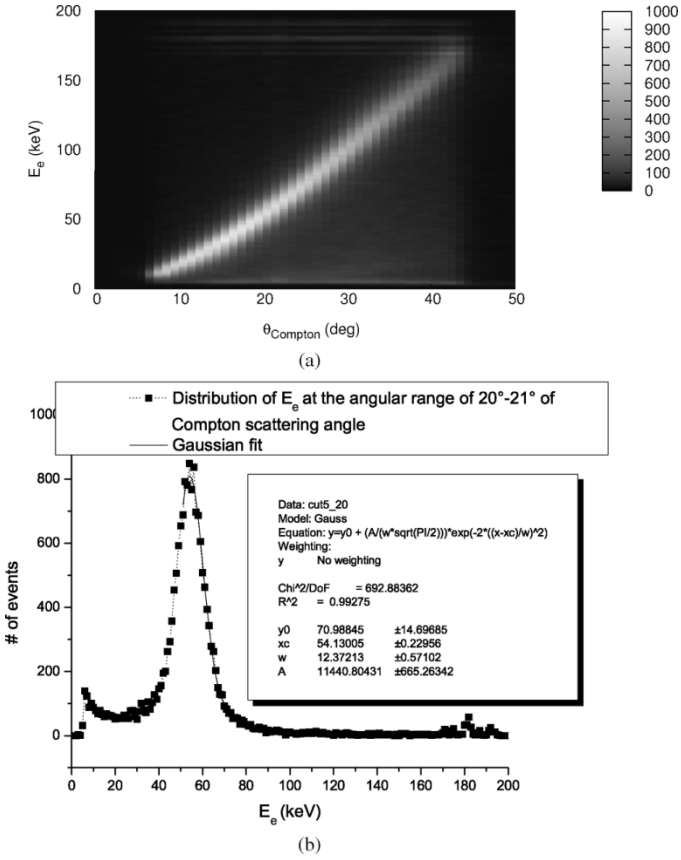

Fig. 7. The energy of the recoil electron measured in the SDD as a function of the Compton scattering angle and the distribution of the E_e at a fixed scattering angle. (a) E_e versus Compton scattering angle. (b) Distribution of E_e at 20°.

coordinate information of the events occuring in both detectors. The energy of the recoil electron measured in the SDD as a function of the Compton scattering angle which is calculated using the coordinate measurement in the Anger camera is shown in Fig. 6(b). The resulting distribution is located around the expected curve with some other events where mostly the recoil electron is not fully captured in the SDD.

The hole collimator is removed in order to obtain higher statistics of events. Without the hole collimator, the beam spread is around a factor of 10 larger and more SDD cells can be covered by the beam. The Anger camera's orientation is adjusted such that an angular range of 10°–50° is covered for the scattered photons leaving the first detector. The coincidence rate with the readout of 13 SDD channels is around 9 events/10 s which makes the collection of 1M Compton events within 2 weeks possible. Fig. 7(a) shows the two-dimensional (2-D) histogram plot of the distribution of the electron energy measured in the SDD as a function of the scattering angle. The scattering angle is calculated using the position of the coincidence events measured. The distribution of electron energy at 20° of scattering angle is analyzed in Fig. 7(b). The uncertainty in the distribution includes the contributions from the energy resolution, Doppler broadening and coordinate measurements. In addition, binning of the histogram the angular range of consideration is 20°–21°. The tail of the distribution on the left side is due to the partial absorption of the electron energy in the scatter detector resulting from the escape of the recoil electron from this detector.

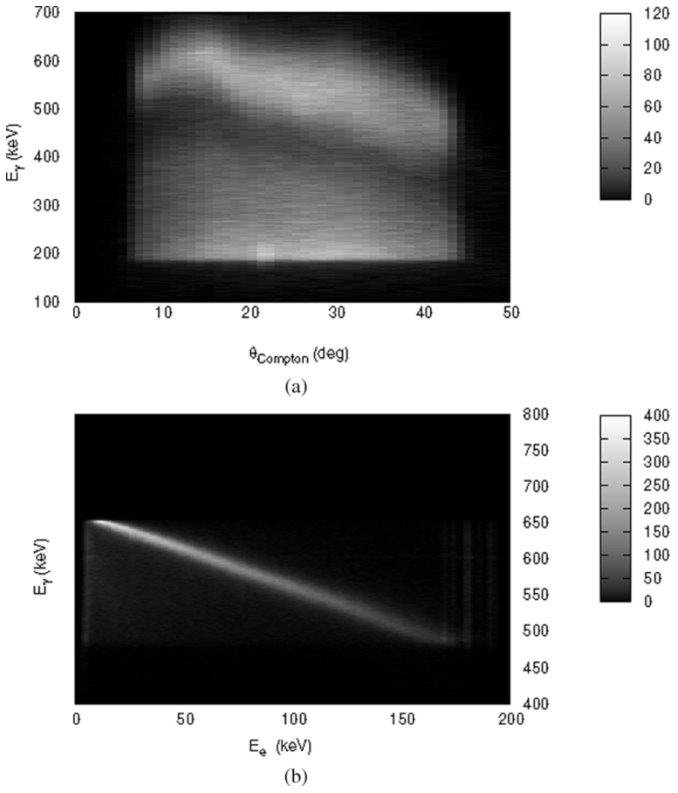

Fig. 8. The energy of the scattered photon measured in the Anger camera as a function of the Compton scattering angle and E_γ as a function of E_e where E_γ is calculated from the scattering angle. (a) E_γ versus Compton scattering angle. (b) E_γ vs E_e.

The energy distribution of the scattered photons measured in the Anger camera as a function of the scattering angle is shown in Fig. 8(a). When Figs. 7(a) and 8(a) are compared, it is clear that the energy measurement in the silicon detector provides much more accurate result than the energy measurement in the Anger camera, as expected. Fig. 8(a) also demonstrates the fact that the fraction of the Compton scattering events in NaI(Tl) is quite high at this energy range. E_γ as a function of E_e is shown Fig. 8(b) where the scattered photon energy is calculated from the scattering angle that is determined using the coordinate information measured in the Anger camera, rather than the energy measured in this detector. The total mean angular resolution and the individual contributions from the system geometry, energy resolution of the scatter detector and the Doppler broadening calculated theoretically for the current system are shown in Fig. 9(a). The energy measured in the scatter detector and the positions of the events measured in both detectors are used for the reconstruction of the point-like source. For the image reconstruction a newly implemented algorithm [11] which is based on the imaginary time expectation maximization (ITEM) algorithm [12] is used. The reconstruction is performed in two steps.

- Preanalysis: a so-called simple backprojection is done with voxels that are large (instead of 1×1, it is started with a 4×4 voxels); the obtained distribution is used for defining different parameters required in the process of reconstruction.

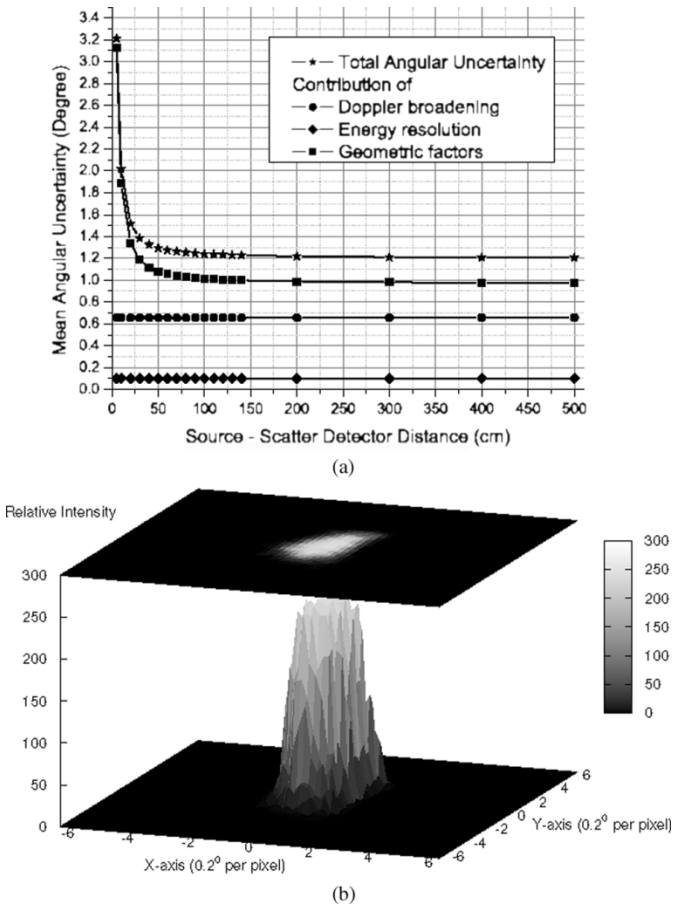

Fig. 9. Mean angular uncertainty calculated theoretically and the reconstructed image for a point source located 120 cm away from the first detector. The FWHM angular uncertainty calculated at this distance is within the expectation limits. (a) Expected angular uncertainty. (b) Reconstructed image.

- Reconstruction: the iterative process starts with the distribution obtained in the preanalysis. A modified projection method together with a Monte Carlo technique is used to improve iteratively a given distribution, i.e., reconstructed image. In this way, one obtains at final iteration the reconstructed 3-D distribution of the sources

The reconstructed image is shown in Fig. 9(b) where the FWHM angular uncertainty corresponds to about 1.4° which is in good agreement with the expected value of the FWHM angular resolution of 1.3°.

IV. Conclusion

A Compton camera test setup has been constructed to study coincidence events and to compare the measurements with existing simulation results. The recent results obtained with this system are compiled in this paper. Energy and position measurement results presented above shows that it is possible to reconstruct Compton events for monoenergetic source distributions using a silicon drift detector with excellent energy resolution and an absorption detector with reasonable position resolution even if the scattered photon energy is only partially absorbed. The present system can be improved by using a stack of silicon detectors as a scatter detector [10]. Such

an improved system would have potential applications in the fields of safety inspection, material science, portal imaging, astrophysics, and nuclear tracer methods in biomedicine and nuclear medicine.

REFERENCES

[1] W. L. Rogers, N. H. Clinthorne, and A. Bokozdynia, *Compton cameras for nuclear medical imaging*.

[2] V. Schönfelder, "Lessons learnt from COMPTEL for future telescopes," *New Astronomy Rev.*, vol. 48, pp. 193–198, 2004.

[3] J. B. Martin, N. Dogan, J. E. Gormley, G. F. Knoll, M. O'Donnell, and D. K. Wehe, "Imaging multi-energy Gamma-ray fields with a Compton scatter camera," *IEEE Trans. Nucl. Sci*, vol. 41, no. 4, pp. 1019–1025, 1994.

[4] T. Çonka Nurdan, K. Nurdan, F. Constantinescu, B. Freisleben, N. A. Pavel, and A. H. Walenta, "Impact of the detector parameters on a Compton camera," *IEEE Trans. Nucl. Sci.*, pt. 1, vol. 49, no. 3, pp. 817–821, Jun. 2002.

[5] T. Çonka Nurdan, "High resolution measurements with silicon drift detectors for compton camera applications," Ph.D. dissertation, Univ. Siegen, Phys. Dep., Jan. 2005.

[6] T. Çonka Nurdan, K. Nurdan, A. H. Walenta, H. J. Besch, C. Fiorini, B. Freisleben, and N. A. Pavel, "Silicon drift detector readout electronics for a Compton camera," *Nucl. Instr. Meth. A*, vol. 523, pp. 435–440, 2004.

[7] T. Çonka Nurdan, K. Nurdan, K. Laihem, A. H. Walenta, C. Fiorini, N. Hörnel, L. Strüder, and C. Venanzi, "Compton electrons in silicon drift detector: first results," in *Proc. IEEE Nuclear Science Symp. and Medical Imaging Conf. 2003*, Portland, OR, Oct. 19–26, 2003.

[8] K. Nurdan, H. J. Besch, T. Çonka-Nurdan, B. Freisleben, N. A. Pavel, and A. H. Walenta, "FPGA based data acquisition system for a Compton camera," in *Proc. SAMBA (Symp. Applications of Particle Detectors in Medicine, Biology and Astrophysics) II*.

[9] T. Çonka Nurdan, K. Nurdan, K. Laihem, A. H. Walenta, C. Fiorini, B. Freisleben, N. Hörnel, N. A. Pavel, and L. Strüder, "Preliminary results on Compton electrons in silicon drift detector," *IEEE Trans. Nucl. Sci.*, vol. 51, no. 5, pp. 2526–2532, Oct. 2004.

[10] A. H. Walenta, A. Brill, A. Castoldi, T. Çonka Nurdan, C. Guazzoni, K. Hartmann, A. Longoni, K. Nurdan, and L. Strüder, "Vertex detection in a stack of Si-drift detectors for high resolution Gamma-ray imaging," *IEEE Trans. Nucl. Sci*, vol. 52, no. 5, Oct. 2005.

[11] I. Chiosa, "New implementation of a compton camera image reconstruction algorithm for biomedical applications," M.Sc. thesis, Univ. Siegen, Phys. Dep., Jul. 2004.

[12] J. Pauli, E. M. Pauli, and G. Anton, "ITEM—QM solutions for EM problems in image reconstruction exemplary for the Compton camera," *Nucl. Instr. Meth. A*, vol. 488, pp. 323–331, 2002.

[13] K. Nurdan, H. J. Besch, T. Çonka-Nurdan, B. Freisleben, N. A. Pavel, and A. H. Walenta, "FPGA based data acquisition system for a Compton camera," *Nucl. Instr. Meth. A*, vol. 510, no. 1–2, pp. 122–125, 2003.